

Otkedma Axoke

Department of Physics,
Faculty of Science,
University of Zululand,
KwaDlangezwa 3886,
SOUTH AFRICA

Preparation and Structural Characterization of $\text{Cu}_2\text{ZnSnS}_4$ Thin Films by Quenching-Assisted Coating Method

In this work, the role of substrate temperature on the structure and microstructure of $\text{Cu}_2\text{ZnSnS}_4$ thin films was investigated. The results showed that the structure was amorphous for as-deposited films while it was polycrystalline for films prepared at elevated temperature. The grain size decreased while roughness increased with increasing substrate temperature. The obtained results gave indication that there is a relation between the structure and preparation temperature as well as heat treatment.

Keywords: $\text{Cu}_2\text{ZnSnS}_4$ semiconductor; Thin films; Heterojunction; Quaternary compounds

1. Introduction

A promising candidate for low cost absorber layers is the quaternary compound $\text{Cu}_2\text{ZnSnS}_4$ (CZTS) which is an analogue of CuInS_2 (CIS) obtained by replacing In(III) by Zn(II) and Sn(IV) in a 50:50 ratio. This direct bandgap p-type semiconductor [4], which has received remarkably little attention in the literature, contains only abundant non-toxic elements. The band gap values reported for CZTS (1.45-1.6 eV) [5-7] fall within the optimum range for a single junction terrestrial solar cell. CZTS has been prepared by Katagiri and co-workers, who used inline vacuum sputtering of Cu, SnS and ZnS followed by annealing in a hydrogen sulfide atmosphere [5,8]. Initial attempts to fabricate photovoltaic devices with these CZTS films led to promising results, with AM 1.5 efficiencies of up to 5.7% [5].

The quaternary compounds (CuZnSeTe , CuZnSeS and $\text{Cu}_2\text{ZnSnS}_4$) are considered as absorbing materials for solar cell applications. There are few data available about their bulk material properties [1-3] as well as thin films [4-7]. The available data refer that there is a strong dependence between their structure and preparation conditions, which may be due to the amorphous nature as well as the dependencies of their properties on the ambient conditions. The electrical properties and optical properties for $\text{Cu}_2\text{ZnSnS}_4$, CuZnSeTe and CuZnSeS thin films were intensively studied [8-13].

CZTS whose crystal structure is shown in Fig. (1) is promising as it replaces rare and expensive In, Ga in commercial $\text{CuIn}_x\text{Ga}_{(1-x)}\text{Se}_2$ (CIGS) solar cells with earth-abundant and cheap Zn, Sn, which could reliably support terawatt renewable electricity consumption [14]. Meanwhile it shares similar properties with CIGS. CZTS at this stage mainly imitates the processing of CIGS as a shortcut for development. Co-evaporation is proved a successful technique in achieving the record 21.7% CIGS solar

cell efficiency [15]. Besides this, sequential evaporation of the elements or compound often shows strong inhomogeneity and multi-phases [16]. Additionally, a close to stoichiometry pure sulphide CZTS solar cell has achieved 4.1% by one step co-evaporation without further sulfurization [17]. Moreover, chemical composition is one of the major factors to influence efficiency [18]. Therefore, co-evaporation of CZTS and chemical composition inhomogeneity of the evaporated film is continuously investigated.

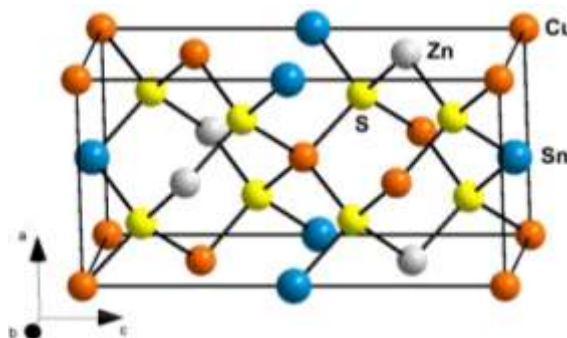


Fig. (1) Crystal structure of $\text{Cu}_2\text{ZnSnS}_4$

Chemical composition non-uniformity is not an issue for CIGS solar cell, however may form a major challenge for CZTS solar cells. CIGS has a wide range of tolerance of the anion-to-cation off-stoichiometry [19]. However, CZTS has a narrow chemical composition window for a single phase CZTS absorber [20]. Meanwhile, empirically a sweet chemical range for high efficiency CZTS solar cells has been identified: ratio of $\text{Cu}/(\text{Zn}+\text{Sn})=0.8-0.9$ and $\text{Zn}/\text{Sn}=1.2-1.3$ [18]. It implies the tolerance for the composition variation: $(0.9-0.8)/0.8=12.5\%$ for $\text{Cu}/(\text{Zn}+\text{Sn})$ and $(1.3-1.2)/1.2=8.33\%$ for Zn/Sn . As Cu/Sn ratio appears to be also important [21], it was also included in this study. Even at compositions in this range, the efficiencies reported by different

groups could have a difference above 10% [18]. This paper is to reveal whether composition uniformity is an issue for future CZTS production [22,23].

This work is devoted to perform quaternary alloy of $\text{Cu}_2\text{ZnSnS}_4$ and then to prepare thin films at various substrate temperatures and point out the dependencies of dielectric and structural properties on deposition condition using relation between the preparation temperature and these properties.

2. Experimental Part

The alloys of $\text{Cu}_2\text{ZnSnS}_4$ were prepared by quenching technique. The exact amounts of high purity (99.999%) copper (Cu), zinc (Zn), selenium (Se) and sulphur (S) were used to form mixtures. These mixtures were sealed in quartz ampoules evacuated down to 10^{-3} torr. These ampoules containing the mixtures were heated up inside a furnace to 1000°C and frequently rocked at the highest temperature for 10 hours. The quenching step was carried out in water immediately after taking out the ampoules from the furnace. The $\text{Cu}_2\text{ZnSnS}_4$ thin films were deposited on substrates of different temperatures ($30, 100,$ and 150°C) using an Edward vacuum coating system.

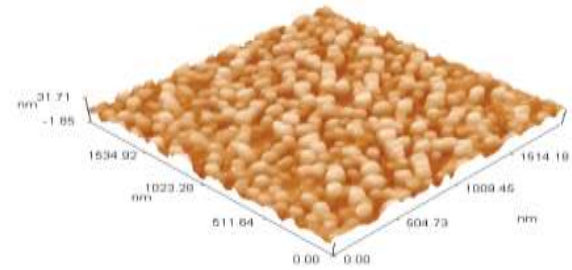
The structural properties of the prepared $\text{Cu}_2\text{ZnSnS}_4$ films were studied using Shimadzu XRD-6000 X-ray diffractometer. The microstructure of the deposited films was also examined using AA3000 atomic force microscope and structural parameters such as crystallite size and roughness were obtained. The Debye-Scherrer's formula was used to calculate crystallite size of the deposited film as follows

$$D = \frac{0.9\lambda}{\beta \cos\theta} \quad (1)$$

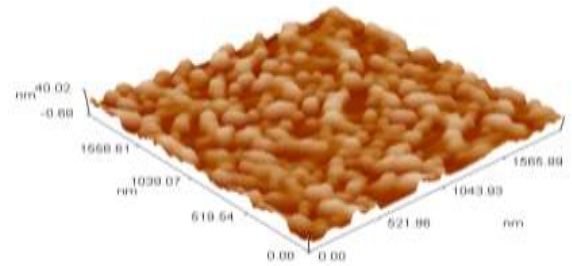
where λ is the wavelength of the x-ray beam, β is the FWHM in radians and θ is the diffraction angle

3. Results and Discussion

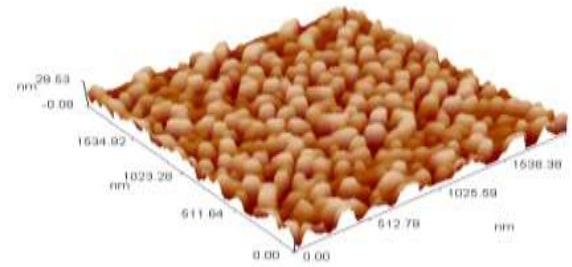
The AFM images of the $\text{Cu}_2\text{ZnSnS}_4$ thin films deposited on a substrate with temperatures of $30, 100$ and 150°C , respectively, are shown in Fig. (2). It was found that the amorphous structure lead to decrease the reflectance, and hence to decrease the density. Therefore, a local increase in film thickness is obtained. The crystallization occurs at elevated temperatures (100 and 150°C), which is related to the reflectance increment and hence increase in film density. The well-pronounced single phase of $\text{Cu}_2\text{ZnSnS}_4$ at high substrate temperature (150°C) has produced much more dense crystallites arranged vertically with a size of 5.25 nm of the film. At elevated temperatures, the grain sizes decrease and exhibit much more homogeneous distribution. Table (1) summarizes the average grain size and average roughness of the prepared $\text{Cu}_2\text{ZnSnS}_4$ thin films.



(a) 50°C



(b) 100°C



(c) 150°C

Fig. (2) AFM images of $\text{Cu}_2\text{ZnSnS}_4$ thin films deposited at different substrate temperatures ($50, 100$ and 150°C)

Table (1) The average grain size and average roughness of the prepared $\text{Cu}_2\text{ZnSnS}_4$ thin films

T_s ($^\circ\text{C}$)	Grain size (nm)	Average roughness (nm)
50	66.29	3.42
100	80.53	4.73
150	77.92	5.25

Figure (3) shows the x-ray diffraction (XRD) pattern for $\text{Cu}_2\text{ZnSnS}_4$ alloy, which exhibits sharp peaks at 2θ of $27.492^\circ, 27.969^\circ, 32.027^\circ, 43.004^\circ$ and 46.291° corresponding to the reflection from (212), (111), (200), (110) and (220) planes, respectively. These reflections represent a hexagonal structure.

The XRD patterns of $\text{Cu}_2\text{ZnSnS}_4$ films prepared at different substrate temperatures ($50, 100$ and 150°C) are plotted in Fig. (4). They reveal no peaks and confirmed the amorphous structure of the as-deposited films. At elevated substrate temperatures, figure (3) shows many peaks located at 2θ of $32.346^\circ, 43.431^\circ$ and 66.649° , which correspond to the reflection from (202), (213) and (215) planes, respectively, and at 27.758° corresponding to the

reflection from (311) plane for samples deposited at the same substrate temperature. These reflections represent a tetragonal structure for samples deposited at substrate temperature of 100 and 150°C.

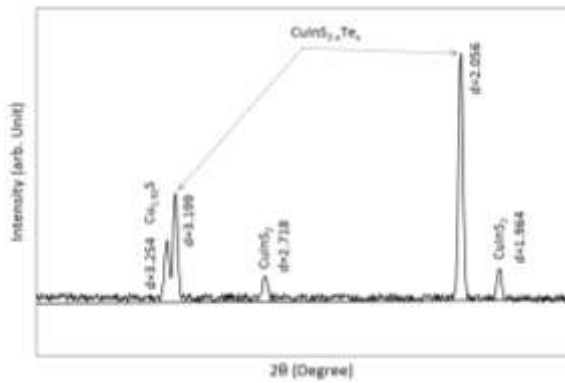


Fig. (3) The XRD pattern for $\text{Cu}_2\text{ZnSnS}_4$ powder extracted from films deposited on substrates

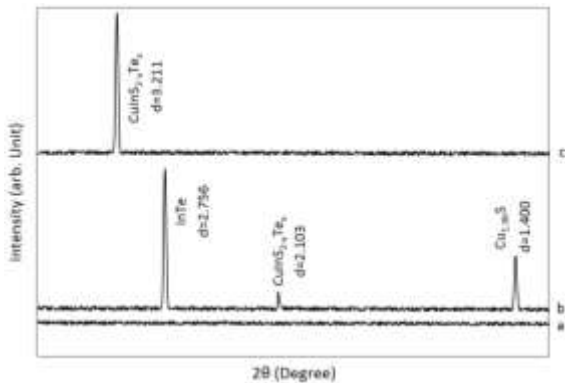


Fig. (4) The XRD patterns for $\text{Cu}_2\text{ZnSnS}_4$ thin films of 700nm thickness deposited at different substrate temperatures (a) 50°C, (b) 100°C and (c) 150°C

It can be concluded that the substrate temperature plays an important role in the structure behavior. Also, it is clear that the orientation of crystal peaks are low and weak at low temperature range (20-100°C), often found binary material such as CuS and ZnSn. By Comparing to high substrate temperatures, it is clearly defined and observed the sharp peaks, especially for the principal peaks on the quaternary $\text{Cu}_2\text{ZnSnS}_4$ compound of chalcopyrite structure oriented along the crystal plane (311) that located at 2θ of 27.783°. Since, there are no standard values available for $\text{Cu}_2\text{ZnSnS}_4$ compound, the XRD peaks are indexed and compared with the data of Landry et al. [24]. From table (2), the inverse relation between the grain size (D) and dislocation density (δ) can be observed. On the other hand, the grain size of $\text{Cu}_2\text{ZnSnS}_4$ samples deposited at 100°C (63.1 nm) is larger than that of $\text{Cu}_2\text{ZnSnS}_4$ powder 35.3 nm, while D of $\text{Cu}_2\text{ZnSnS}_4$ sample suffer abrupt reduction from 49.4 to 3.31 nm for sample deposited at 150°C. It is worthy to note that the comparison is done between

the diffraction peaks that located at 32.346° and 27.647°.

Table (2) The X-ray diffraction data 2θ , d , $(I/I_0)_{exp}$, δ , FWHM and D for $\text{Cu}_2\text{ZnSnS}_4$ powder and 700nm thin films deposited at different substrate temperatures (50, 100 and 150°C)

Samples	$2\theta_{exp}$ (deg)	d_{exp} (Å)	$(I/I_0)_{exp}$	FWHM (deg)	D (Å)	$\delta \times 10^5$ (Å) ⁻²
powder	27.492	3.254	23%	0.1956	417.58	0.573
	27.969	3.199	43%	0.1655	494.79	0.408
	32.027	2.718	9%	0.2346	353.26	0.801
	43.004	2.056	100%	0.1620	529.11	0.357
	46.291	1.964	13%	0.1774	487.02	0.422
Films $T_s=50^\circ\text{C}$	Amorphous					
Films $T_s=100^\circ\text{C}$	32.346	2.756	100%	0.1310	631.89	0.25
	43.431	2.103	9%	0.1700	503.41	0.394
	66.649	1.400	39%	0.2873	331.22	0.911
Films $T_s=150^\circ\text{C}$	27.647	3.211	100%	2.4675	33.180	9.1

Figure (5) shows the scanning electron microscopy (SEM) images for $\text{Cu}_2\text{ZnSnS}_4$ alloy samples deposited as thin film on substrates of different temperatures (50, 100 and 150°C). It is clear that the surface of the $\text{Cu}_2\text{ZnSnS}_4$ film deposited at substrate temperature of 50 °C is containing of particles with inhomogeneous distribution of both size and density. As well, the polycrystalline structure is confirmed in accordance to the XRD pattern of this sample. Some voids are also observed due to the inefficient alloying step of the quaternary compound during the deposition process. For the $\text{Cu}_2\text{ZnSnS}_4$ film deposited at substrate temperature of 100 °C, the differences in particle sizes are much more apparent while the particles get larger and increasingly diffused together. The inhomogeneity in particle size and density over the film surface is apparently higher, which is attributed to the effect of higher temperature of the substrate on which the film is deposited. Due to small thickness of the deposited $\text{Cu}_2\text{ZnSnS}_4$ film and the thermal effect associated to increasing substrate temperature, the growth of certain crystal planes increases whereas the growth of other crystal planes is limited or restricted. Therefore, the surface exhibits higher degree of roughness in agreement to the AFM result. As the substrate temperature is increased to 150 °C, the interstitial voids are reasonably disappeared due to the higher diffusion between particles showing higher inhomogeneity in size and distribution. Consequently, the surface roughness is decreased in agreement to the AFM result as the vacancies over the polycrystalline structure are filled with smaller particles and hence lowering the difference between the highest and lowest points over the surface.

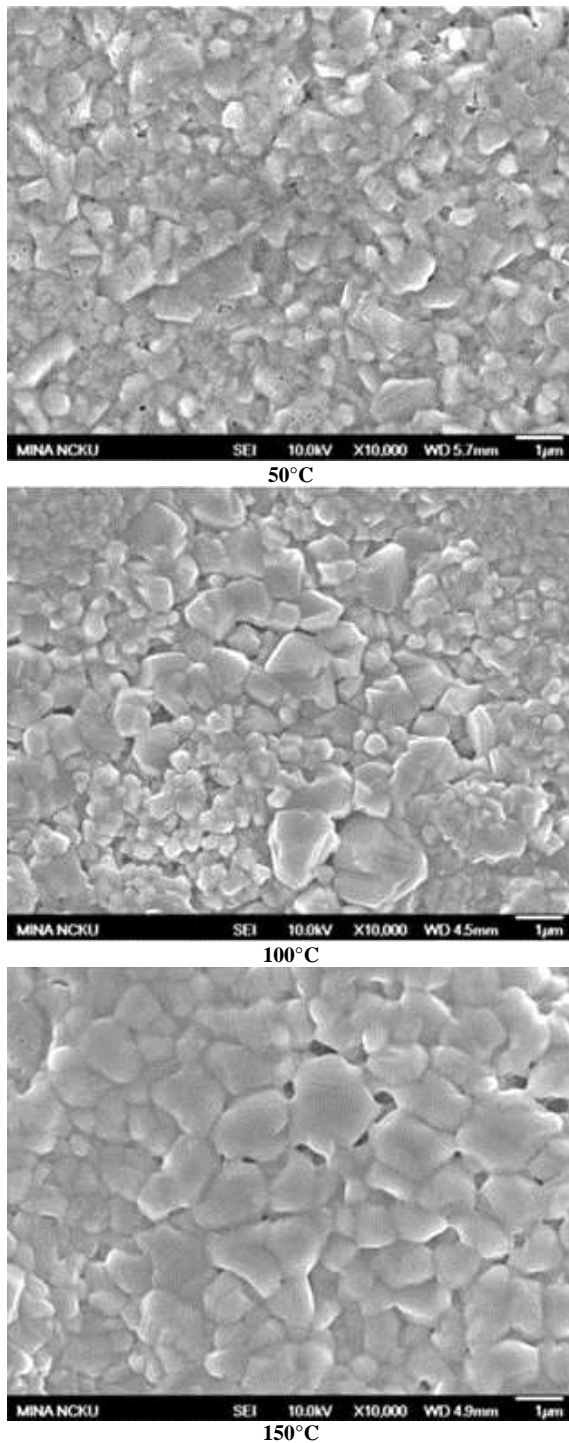


Fig. (5) The SEM images for $\text{Cu}_2\text{ZnSnS}_4$ powder extracted from films deposited on substrates of different temperatures

4. Conclusions

From the results obtained from this work, it can be concluded that the single phase with chalcopyrite structure of $\text{Cu}_2\text{ZnSnS}_4$ becomes more pronounced at elevated temperatures.

References

- [1] B.A. Hasan and D.A. Umran, *Semicond. Sci. Technol.* 27 (2012) 125014(6pp).
- [2] B.A. Hasan, *Int. J. Thin Film Sci. Tech.*, 2(1) (2013) 29-36.
- [3] R. Diaz, M. Leon, and F. Reuda, *J. Vac. Sci. Technol. A* 10 (1992) 295-300.
- [4] K. Inakoshi, T. Ohashi, Y. Hashimoto, and Kentaro Ito, *Solar Energy Mater. Solar Cells*, 50(1) (1998) 37-42.
- [5] K. Subbaramiah and V. Sundara Raja, *Thin Solid Films*, 208 (1992) 247-251.
- [6] T. Ohashi, A. J. Ger, T. Miyazawa, Y. Hashimoto and K. Ito, *Jap. J. Appl. Phys.*, 34 (1995) 4159-4166.
- [7] S. Kuranouchi and T. Nakazawa, *Solar Energy Mater. Solar Cells*, 50 (1998) 31-36.
- [8] L.I. Soliman and T.A. Hendia, *Rad. Phys. Chem.*, 50(2), 1997, 175-177.
- [9] L. Soliman, T. Hendia and H. Zayed, *Fizika A (Zagreb)*, 16(1) (2007) 39-46.
- [10] J.Y.W. Seto, *J. Electrochem. Soc.*, 122(5) (1975) 701-706. doi: 10.1149/1.2134296
- [11] S. Kumar, B. Prajapati, S. Tiwari and V. Tiwari, *Indian J. Pure Appl. Phys.*, 46 (2008) 198-203.
- [12] A.K. Jonscher, *J. Phys. D: Appl. Phys.*, 32(14) (1999) R57-R70. DOI: 10.1088/0022-3727/32/14/201
- [13] Z. Ahmad, "**Polymeric Dielectric Materials**", Ch. 1 (2014) p. 4, doi: 10.5772/50638.
- [14] L.M. Peter, *Phil. Trans. Royal Soc. of London A: Math. Phys. Eng. Sci.*, 369(1942) (2011) 1840-56.
- [15] M.A. Green et al., *Prog. in Photovolt.*, 22(1) (2014) 1-9.
- [16] B.A. Schubert et al., "An economic approach to evaluate the range of coverage of indium and its impact on indium based thin-film solar cells—recent results of $\text{Cu}_2\text{ZnSnS}_4$ ", 23rd EU-PVSEC; 2008; Valencia.
- [17] B.-A. Schubert et al., *Prog. in Photovolt.: Res. Appl.*, 9(1) (2011) 93-6.
- [18] D.B. Mitzi et al., *Sol. Ener. Mater. Sol. Cells.*, 95(6) (2011) 1421-36.
- [19] K.L. Chopra, P.D. Paulson and V. Dutta, *Prog. in Photovolt.: Res. Appl.*, 12(2-3) (2004) 69-92.
- [20] S. Chen et al., *Appl. Phys. Lett.*, 96(2) (2010) 021902.
- [21] C. Yan et al., *J. Alloys Comp.*, 610 (2014) 486-91.
- [22] R. Bari and L. Patil, *Sens. Transd.*, 125 (2011) 213-219.
- [23] S. Sze and K. Kwok, "**Physics of Semiconductor Devices**", 3rd ed., John Wiley & Sons, Inc. (New Jersey, 2007).
- [24] C. Landry, J. Lockwood and R. Barron, *Chem. Mater.* 7(4) (1995) 699-706.